

Photo-Oxidative Degradation of Polypropylene Nanocomposites - Effect of Incorporation of Additives on Performance Characteristics

Kadambanathan. K, Chandrasekar. K, Muthukumar. K

Mailam Engineering College, Mailam, Tamil Nadu, India

ABSTRACT

In the present work, polypropylene (PP)/C20A nanocomposite films were prepared in a blown film extruder. Commercially modified organoclay, Cloisite 20A (C20A) and polypropylene grafted maleic anhydride (PP-g-MA), was used as a reinforcing agent and compatibilizer respectively for the preparation of nanocomposites films. To improve the photo-oxidative degradation of PP/nanocomposite films two different photo initiators; commercial grade ferrocene and iron ricinoleate (synthesized from castor oil) has been added to the nanocomposites films. FTIR analysis of the irradiated samples containing ferrocene and iron ricinoleate shows improved photo oxidative characteristics as compared to PP clay nanocomposites films. Mechanical characterization showed decreased tensile strength, tensile modulus and tear resistance of PP nanocomposites as compared to virgin matrix. However with the addition of PP-g-MA, an improvement in the mechanical properties was obtained due to the particle size reduction of silica agglomerates. Thermal analysis has been carried out employing differential scanning calorimetry (DSC) and thermo gravimetric analysis (TGA). An increase in the degree of crystallinity of PP nanocomposites with the increase in exposure time period in UV has been observed. TGA thermograms also indicated that the thermal stability of exposed samples were higher than those of the unexposed samples.

Keywords: Ferrocene, FTIR, Carbonyl index, TGA, Castor oil

I. INTRODUCTION

The volume of domestic and industrial waste has been increased almost exponentially in the recent years. This has in turn lead to serious environmental threat, owing to limited availability of landfills in the vicinity areas of large cities and industries (1, 2). Plastic materials represent a significant volume of the solid waste due to their relative low density and these wastes remain intact in nature for more than 50 years in the landfills and sites. Several attempts have been made to either decrease the volume of plastic waste or to enhance the degradation process in these materials by the introduction of various photodegradable additives (3). Protection of the environment has been one of the main driving forces which sustain interest in these photodegradable polymers. The simplest method of promoting photo degradation in the polymers is to introduce photo initiators such as metal salts and benzophenone derivatives into polymer films (4).

There are many factors influencing the degradation of polymeric materials, such as photo-irradiation, thermo-degradation, oxidation, hydrolysis etc. Within the various factors, photo-oxidative degradation tends to change in chemical structures, physical properties and appearance of a plastic. Thus, the study on photo-oxidative degradation of polymeric materials has gained considerable importance in the field of polymer degradation and stability (6). Further polymer layered silicate nanocomposites (PLSN) research has attracted substantial interests in the recent years. Compared to the conventional filled polymers, PLSN have many unique properties in the presence of a small amount of layered silicate, such as enhanced mechanical properties, increased heat distortion temperature, improved thermal stability, decreased gas and vapor permeability and reduced flammability characteristics (7-13).

II. METHODS AND MATERIAL

2. Experimental Procedure

2.1 Materials

Isotactic polypropylene (PP-Extrusion grade) having density of 0.92 g/cc and MFI of 10gm/10min obtained from M/s Reliance Industries Ltd., Mumbai, India has been used as the base polymer matrix. The organoclay used in this study (Cloisite20A) is supplied by M/s Southern Clay Products (Gonzales, TX, USA). It is a Na^+ montmorillonite, chemically modified with dimethyl dehydrogenated tallow quaternary ammonium chloride (Cation exchange capacity (CEC) of 95 meq/100 g), where N^+ denotes quaternary ammonium chloride and HT denotes hydrogenated tallow (Fig. 1). HT is made of approximately 65% $\text{C}_{18}\text{H}_{37}$, 30% $\text{C}_{16}\text{H}_{33}$ and 5% $\text{C}_{14}\text{H}_{29}$.



Figure 1. Chemical structure of the dimethyl dihydrogenated tallow quaternary ammonium chloride

Polypropylene-grafted-maleic anhydride (PP-g-MA) containing 1 wt% of maleic anhydride with acid number 8, Brookfield viscosity of 60,000 cp at 190°C and softening point of 158°C was procured from M/s Eastman Chemicals, USA and has been used as a compatibilizer. Ferrocene ($\text{Fe}(\text{C}_5\text{H}_5)_2$), an organometallic compound with a density of 2.69 g/cm³ at 20°C, boiling point, 249°C and melting point 149°C respectively has been used as a Photoinitiator. Iron ricinoleate, was manually prepared from castor oil Castor oil was obtained from local sources.

2.2 Synthesis of iron ricinoleate (Castor oil based additive)

In the present investigation, castor oil containing 95% of ricinoleic acid has been used as an alkenoic fatty acid to synthesize the photoinitiator. The fatty acid was refluxed with 1N NaOH solution over water bath at 80°C in presence of glycerol and excess methanol, for one hour. Subsequently, sodium salts of alkenoic fatty acid was treated with ferric ammonium sulphate to obtain ferric salt of ricinoleic acid which was finally washed

several times with water and dissolved in alcohol at 50°C for 3hrs to obtain pure iron ricinoleate.

2.3 Preparation of PP/Clay nanocomposite films

Table 1. Composition of PP/Clay nanocomposites

Sam ple	Polyprop ylene	PP- g- MA	Cloisite 20A	Ferro cene	Iron Ricinol eate
	(wt. %)	(wt. %)	(wt.%)	(wt%)	(wt.%)
PP	100	-	-	-	-
PP1	97	-	3	-	-
PP2	95	-	5	-	-
PP3	90	5	5	-	-
PP4	87	5	5	3	-
PP5	87	5	5	-	3

2.4 Tensile Properties

Specimens of dimension 25mm x 120mm were taken for measurement of tensile properties in Universal testing machine, (M/s LR. 100K Lloyds Instruments Ltd, UK) as per ASTM D882. The test was carried out at a gauge length of 50 mm and the speed of 500 mm/min.

2.5 Tear resistance

Tear resistance of the films of dimensions 101.60 mm x 19.05mm and 0.750" rad were measured in accordance with ASTM D 1922 in pendulum tear tester(ATSFaar vignate MI, Italy) with a maximum load of 920g.

The samples for mechanical tests were conditioned at 23°C ±2°C and 55%RH before testing and 10 replicate specimens were used for each test. The data reported are average of ten tests.

2.6 UV exposure test

UV exposures were carried out in a weatherometer (ATLAS UV 2000, USA) in accordance with ASTM D-4329-99. The weatherometer chamber was operated using various cycles of exposure, consisting of 8 hrs UV irradiation at (60 ± 1)°C, 4 hrs condensation cycle at (50 ± 1)°C cycle respectively. Subsequently, film

samples of the nanocomposites along with the virgin matrix, were irradiated at a (dose) rate of 0.63 W/m² and wavelength of 300 nm. The distance from the sample to the axis of the lamp was maintained at 10 cm.

III. RESULTS AND DISCUSSION

3. Results and Discussion

3.1 Mechanical properties

The mechanical properties of the unexposed nanocomposites films such as tensile strength, tensile modulus, elongation at break and tear resistance have been evaluated in both machine and transverse direction and the corresponding data is presented in Table 2.

Table 2. Mechanical properties of PP/Clay

S.No	Sample	Tensile strength(N/mm ²)		Tensile modulus(MPa)		Elongation (%)		Tear resistance(N/mm)	
		M.D	T.D	M.D	T.D	M.D	T.D	M.D	T.D
1	PP	34	29.8	1061.6	1089.01	15.26	4.63	205.19	237
2	PP1	19.7	15.73	739.3	727.52	9.78	3.17	113.87	114.67
3	PP2	13.5	14.73	543.36	657.1	22.93	3.26	113.075	114.67
4	PP3	31.5	29.2	1495.8	1446.36	6.13	3.57	91.735	101.93
5	PP4	34.72	31.25	1434.56	1176.85	6.87	3.43	85.496	93.35
6	PP5	39.975	36.12	1299.95	1376.07	10.57	5.61	64.23	76.542

From the Table 2, it is evident that there is a reduction in tensile strength in both transverse and machine directions of PP in PP1, PP2 and PP3 respectively, with the increase in clay loading from 3-5 wt%, Addition of 3wt% of C20A resulted in significant decrease in tensile strength to the tune of 42% and tensile modulus to 30% in the machine direction.

A similar reduction in tensile strength of PP from 29.8MPa to 15.73MPa and tensile modulus from 1089.01 to 727.52 MPa in transverse direction was also observed.

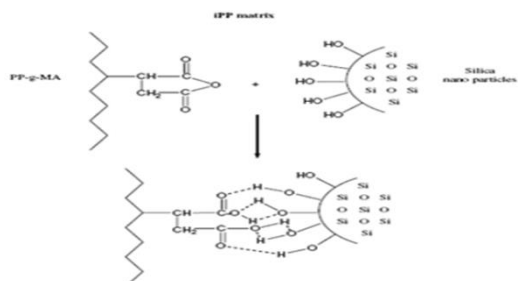


Figure 2. Interaction between the maleic anhydride groups of the grafting agent of PP-g-MA and the surface hydroxyl groups of the silica nanoparticles.

The tensile modulus of polymer nanocomposites depends primarily on the modulus of polymer, and the clay platelets; clay concentration within the matrix

polymer; orientation of the clay tactoids, and polymer crystallites and interfacial stress transfer mechanisms. Test results reported in Table 2, also reveals that there is an additional increase in the mechanical properties of the nanocomposite films with the incorporation of photoinitiators; ferrocene and iron ricinoleate. It is evident that the tensile properties of PP4 and PP5 increased considerably as compared with PP1, PP2 and PP3 as well as virgin PP. The nanocomposite films prepared using 3 wt% of ferrocene showed an optimum increase of tensile strength to 2.5% in transverse direction and 2% in machine direction and tensile modulus to 7% in transverse direction and 26% in machine direction respectively as compared with PP. This behaviour is probably due to reinforcing effect of photoinitiators within the matrix polymer.

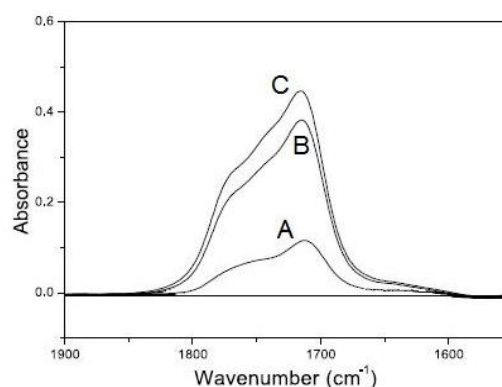


Figure 3. Evolution of infrared spectra of A)PP3 B)PP4 and C)PP5 after 200hr UV exposure in the domain 1900-1500cm⁻¹.

Fig 3 shows the FTIR spectrum PP nanocomposite films exposed in UV beyond 200 hrs time period. It is evident that the absorbance value corresponding to the peak at 1712 cm⁻¹ increases with the addition of clay, ferrocene and iron ricinoleate.(i.e.PP5>PP4>PP3). This behavior is explained in detail in Fig 4, from the respective carbonyl index values of the constituent samples.

Table 3.The TG characterization of PP/clay nanocomposites (before UV exposure)

Sample	T _d (10%) (°C)	T _d (50%) (°C)	Ash% at 700°C
PP	289.7	353.9	0.7
PP1	292.5	354.5	2.32
PP2	300.2	363.4	3.1
PP3	328.3	394.5	2.93
PP4	312.5	385.5	4.95
PP5	328.7	405.6	3.89

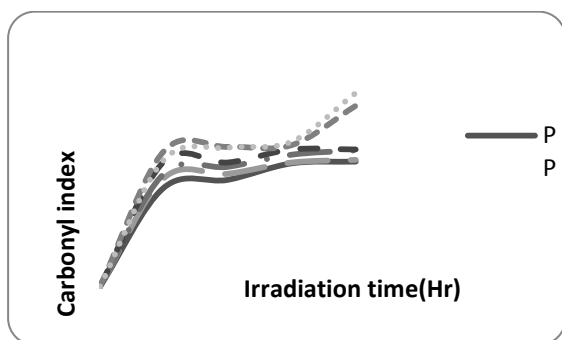


Figure 4. Carbonyl index of the samples

For the quantitative measurement of photo-oxidative degradation, carbonyl index values have been calculated (3) using the following equation:

$$\text{Carbonyl Index} = \frac{\text{Abs } 1712 \text{ cm}^{-1}}{\text{Abs } 2720 \text{ cm}^{-1}}$$

From Fig 4, it is evident that in all the cases, the value of carbonyl index increases with the exposure time. Index values for PP1, PP2 and PP3, loaded with 3 and 5 wt% of C20A nanoclay and 5 wt% of PP-g-MA are comparatively higher than that of virgin PP. The complex crystallographic structure and inherent nature of clay minerals results in creation of catalytic active sites. Also, decomposition of ammonium ions leads to catalytic acidic sites created on the layers and olefin chains. All these photo responsive groups and catalytic active sites accept single electrons from the PP matrix.

Under UV exposure, free radicals formed in the matrix polymer undergo photo-oxidative degradation, which contributes to an overall increase in carbonyl index of PP in the nanocomposite samples.

3.3 Thermo gravimetric analysis (TGA)

The thermal stability of the polypropylene nanocomposite films has been studied using thermo gravimetric analysis. TGA thermograms displayed in Fig.5 shows single step degradation behavior in virgin PP as well as in the nanocomposite films.

One of the parameters that is of interest from the TGA thermograms is the onset of the degradation, which is usually taken as the temperature at which 10% degradation occurs T_d (10%). The data obtained are tabulated in Table 3 and are shown graphically in Fig .5.

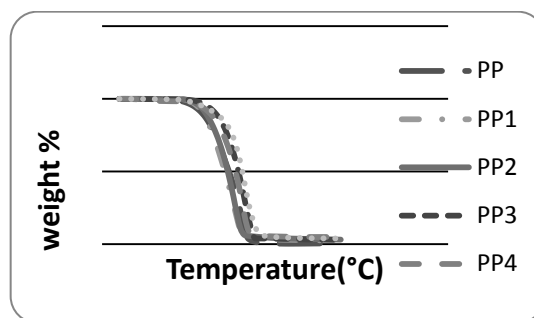


Figure 5. TG curves of unexposed PP/clay nanocomposites.

Test results reported in Fig. 5 and Table 3 shows that, PP nanocomposites exhibit enhanced thermal stability as compared with virgin polymer. At higher clay loading of 3 and 5 wt%, the onset temperature of the nanocomposites are 2.8°C to 10.5°C higher than that of PP. This may be attributed to the presence of inherently thermostable clay layer.

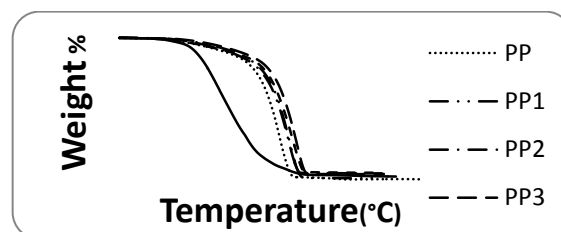


Figure 6. TG curves of UV exposed PP/clay nanocomposites after 200hr.

Table 4. TG characterization of PP/clay nanocomposites (After 200 hrs of UV exposure)

Sample	T_d (10%) (°C)	T_d (50%) (°C)	T_{max} (°C)	Ash% at 700°C
PP	315.5	430	448.08	2.35
PP1	324.5	448.9	469.5	3.1
PP2	337.25	451.5	473.14	6.38
PP3	351.3	468	496.47	5.92
PP4	327.8	458.25	481.53	6.78
PP5	239.87	324.29	298.18	4.327

In general, the major weight losses were obtained in the range of 440°C to 500°C. The maximum weight loss temperature (T_{max}) of PP3, PP4 samples is higher than that of the remaining samples (PP, PP1 and PP2). Particularly, T_{max} of PP3 sample is 496.47°C which is higher than that PP sample by 48°C. The thermal stability of UV degraded nanocomposites

increased with the increase in the content of (C20A) nanoclay from 3 to 5 wt% and the corresponding data are presented in Table 4.

The aforementioned results tabulated in Table 3 and Table 4, also confirmed effectiveness of maleic anhydride (MA) and photoinitiators, on the thermal stability of PP in the nanocomposite films. Presence of MA to the tune of 1 wt. % and its copolymer with polypropylene (PP-g-MA) formed by in-situ melt blending, have dramatically improved the interaction between PP chains and C20A nanoclay, hence the structure of the nanocomposite films becomes more finer with improved dispersion than that without MA. This further result in improved thermal stability in the nanocomposite films.

3.4 Differential scanning Calorimetry

Melting and crystallization behavior of PP nanocomposites with and without photo initiators was monitored as a function of exposure time using DSC. From Fig.7, it is clear that the melting range is shifted to lower temperatures with the increase in degradation.

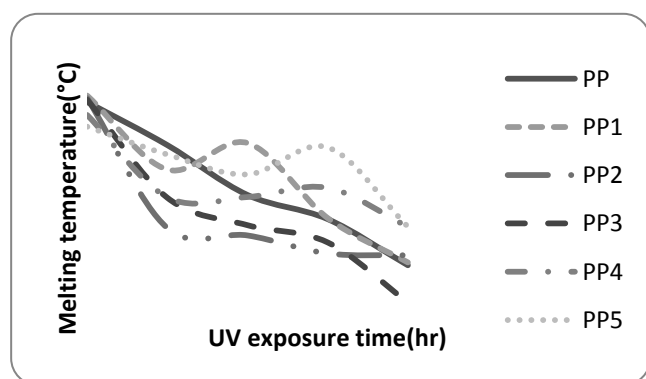


Figure 7. Melting temperature of PP/nanocomposite films as a function of UV exposure time.

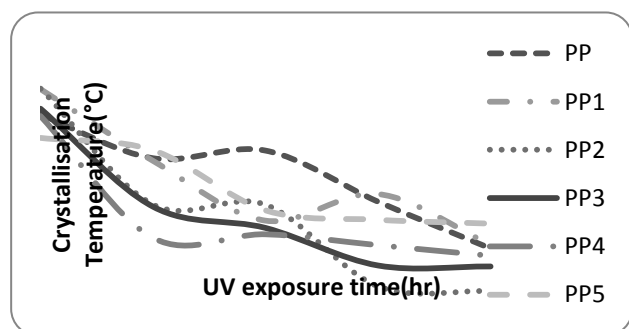


Figure 8. Crystallisation temperature of various PP/nanocomposite films as a function of UV exposure time.

Fig. 8 shows the effect of UV exposure on the crystallization temperature of virgin PP and the nanocomposite films. The crystallization temperature taken as the position of the maximum of the exothermic peak, decreased with exposure time presumably due to the progressively lower molecular weight and larger number of chemical irregularities present in the molecules of the exposed material. It is well known that shorter and defective molecules crystallize more slowly(25,26)

From the Fig. 9, it is evident that crystallinity increases initially with exposure time and then decreases sharply. This behaviour can be associated with two main effect of photodegradation: chain scission and build-up of carbonyl and other impurity groups. So the reduction in molecular size dominates in short exposure time (upto 150hr) which in turn favours the crystallization process.

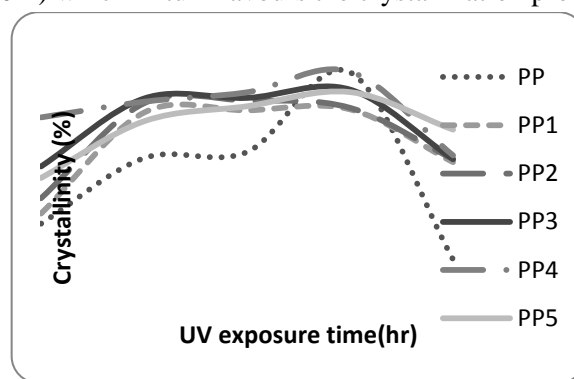


Figure 9. Crystallinity of samples at various UV exposure time.

It also observed that the degree of crystallinity of PP is lower than other samples. All other samples are incorporated with nanoclay and photoinitiators which increases the rate of photo degradation resulting in reduction in molecular size thereby increasing the crystallization process. These oxidation reactions occurs predominantly in the noncrystalline phase and produces small chain segments that crystallize into pre-existing crystal increasing the crystallinity by “chemi-crystallization”.

IV. CONCLUSION

Our present investigation suggests that photo initiators such as ferrocene and iron ricinoleate can considerably improve the photo-oxidative degradation in polypropylene nanocomposites. Among the two photo

initiators, the effect of iron ricinoleate was found to be significant.

Based on our research findings the following conclusions were derived.

- FTIR studies of the films containing ferrocene and iron ricinoleate generate more amounts of carbonyl groups which indicates that the films are more susceptible to UV exposure as compared with other films.
- The synergetic effect of unsaturated C=C bond, iron ion and clay galleries present in the samples containing iron ricinoleate increases the rate of photo-oxidation.
- DSC thermograms show an increase in percentage of crystallinity with increasing exposure time in the nanocomposites films.
- TGA thermograms indicated that UV degraded samples are thermally stable than unexposed samples.
- Corresponding degradation temperature and the ash content in all the UV exposed samples were comparatively higher than that of unexposed samples, thus suggesting the influence of crystal arrangement of matrix polymer in the nanocomposite films, on the thermal properties.
- Mechanical characterization proves that samples containing PP-g-MA exhibit improved mechanical properties as compared to other samples. It is believed that the maleic anhydride groups of PP-g-MA reacts with the surface hydroxyl groups of SiO₂ nanoparticles which results in reduction in size of agglomerates, facilitating improved dispersion.
- Iron ricinoleate, derived from castor oil may improve the biodegradability in the PP based nanocomposites films at optimal concentration. So, the interaction between iron ricinoleate and polyolefins requires further attention in the area of biodegradation because, the initial step for biodegradation depends on photo-oxidation of polyolefins.

V. REFERENCES

- [1] G.scott, "Green' polymers" ,Polymer degradation and stability, 68, 1(2000)
- [2] D.M.wiles and G.Scott, "Polyolefins with controlled environmental degradability", Polymer degradation and stability, 91, 1581(2006)
- [3] G.J.M.Fechine, D.S.Rosa, M.E.Rezende, N.R.Demarquette,"Effect of UV Radiation and Pro-Oxidant on PP biodegradability",Polymer Engineering and Science,2009
- [4] C.David, M.Trojan, A.Daro , "Photodegradation of Polyethylene:comparison of various photoinitiators in natural weathering conditions",Polymer Degradation and stability,37(1992),233-245.
- [5] Michael J.Solomon, Anongnat Somwangthanaroj,"Intercalated Polypropylene Nanocomposites"Dekker Encyclopedia of Nanoscience and Nanotechnology",2004.
- [6] Huaili Qin, Shimin Zhang,Huiju Liu,Shaobo Xie,Mingshu Yang,Deyan," Photo-oxidative degradation of polypropylene/montmorillonite Nanocomposites", Polymer 46 (2005) 3149–3156
- [7] Kojima Y, Usuki A, Kawasumi M, Okada A, Fukushima Y, Kurauchi T, et al. "Mechanical properties of nylon 6-clay hybrid", J Mater Res 1993;8:1185.
- [8] Hotta S, Paul DR.,Nanocomposites formed from linear low density polyethylene and organoclays" Polymer 2004;45:7639.
- [9] Galgali G, Agarwal S, Lele A., "Effect of clay orientation on the tensile modulus of polypropylene–nanoclay composites", Polymer 2004;45:6059.
- [10] Zanetti M, Costa L. "Preparation and combustion behaviour of polymer/layered silicate nanocomposites based upon PE and EVA" Polymer 2004;45:4367.
- [11] Gopakumar TG, Lee JA, Kontopoulou M, Parent JS. "Influence of clay exfoliation on the physical properties of montmorillonite/polyethylene composites", Polymer 2002;43:5483.
- [12] Qin HL, Su QS, Zhang SM, Zhao B, Yang MS. "Thermal stability and flammability of polyamide 66/montmorillonite nanocomposites",Polymer 2003;44:7533.
- [13] Gilman JW. "Flammability and thermal stability studies of polymer layered-silicate (clay) nanocomposites", Appl Clay Sci 1999;15:31.
- [14] Kawasumi M, Hasegawa N, Kato M, Usuki A, Okada A. "Preparation and Mechanical Properties of Polypropylene–Clay Hybrids" Macromolecules 1997;30:6333.
- [15] Manias E, Touny A, Wu L, Strawhecker K, Lu B, Chung TC. "Polypropylene/Montmorillonite Nanocomposites. Review of the Synthetic Routes and Materials Properties" Chem Mater 2001;13:3516.
- [16] Morgan AB, Harris JD. "Effects of organoclay Soxhlet extraction on mechanical properties, flammability properties and organoclay dispersion of polypropylene nanocomposites", Polymer 2003;44:2313.